# Electronic Supplementary Information

# $Mn^{III}$-Peroxo Adduct Supported by a New Tetradentate Ligand Shows Acid-Sensitive Aldehyde Deformylation Reactivity

Melissa C. Denler,[‡a] Gayan B. Wijeratne,[‡a,b] Derek B. Rice,[a] Hannah E. Colmer,[a,c]

Victor W. Day,[a] Timothy A. Jackson*[a]

[a]*The University of Kansas, Department of Chemistry and Center for Environmentally Beneficial Catalysis, 1251 Wescoe Hall Drive, Lawrence, KS 66045, USA.*

[b]*Current address: The University of Alabama at Birmingham, Department of Chemistry, Center for Biophysical Sciences and Engineering, 1025 18th Street South, Birmingham AL 35205*

[c]*Current address: University of Saint Mary, 4100 S 4th Street, Leavenworth, KS 66048, USA.*
[*]*Corresponding author*

‡ The contributions of these authors were of equal merit.

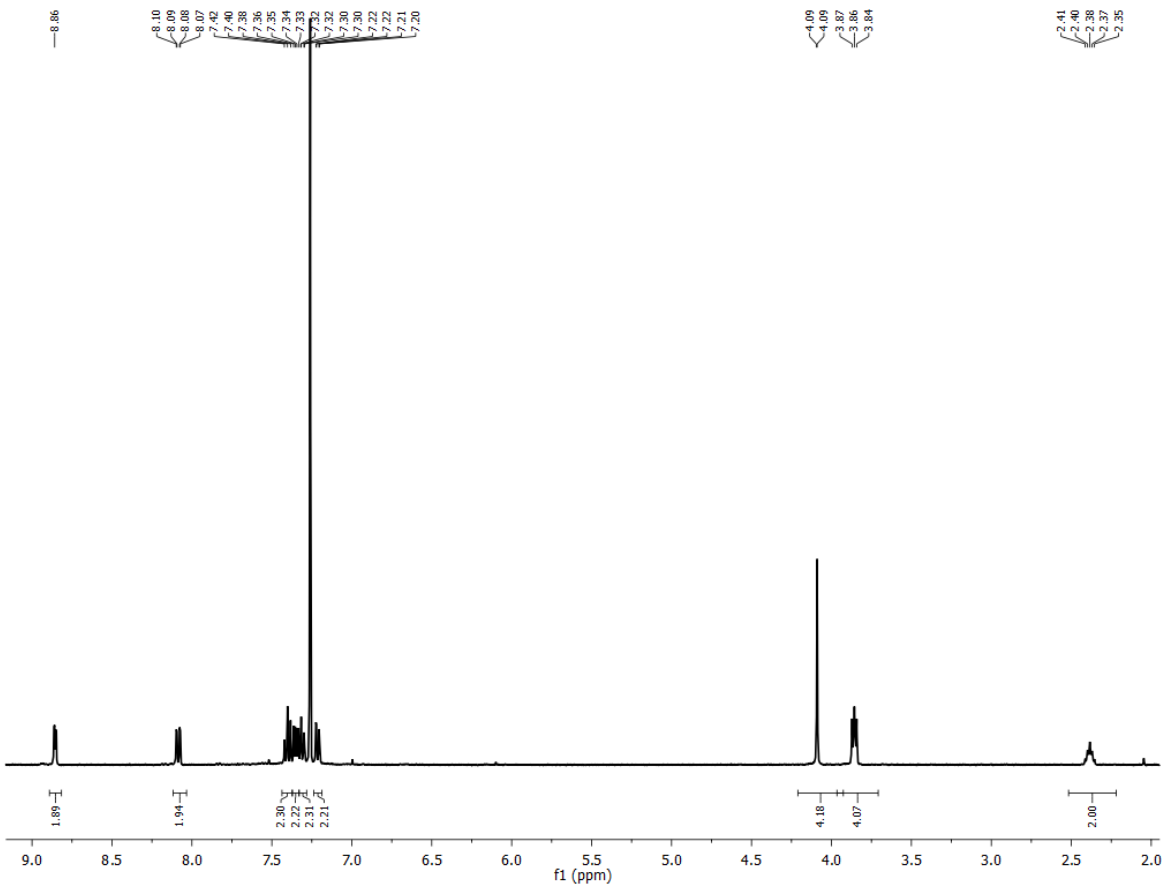


**Figure S1.** $^{1}$H NMR spectrum of the L$^{7}$BQ ligand collected in $CDCl_3$ under ambient conditions.

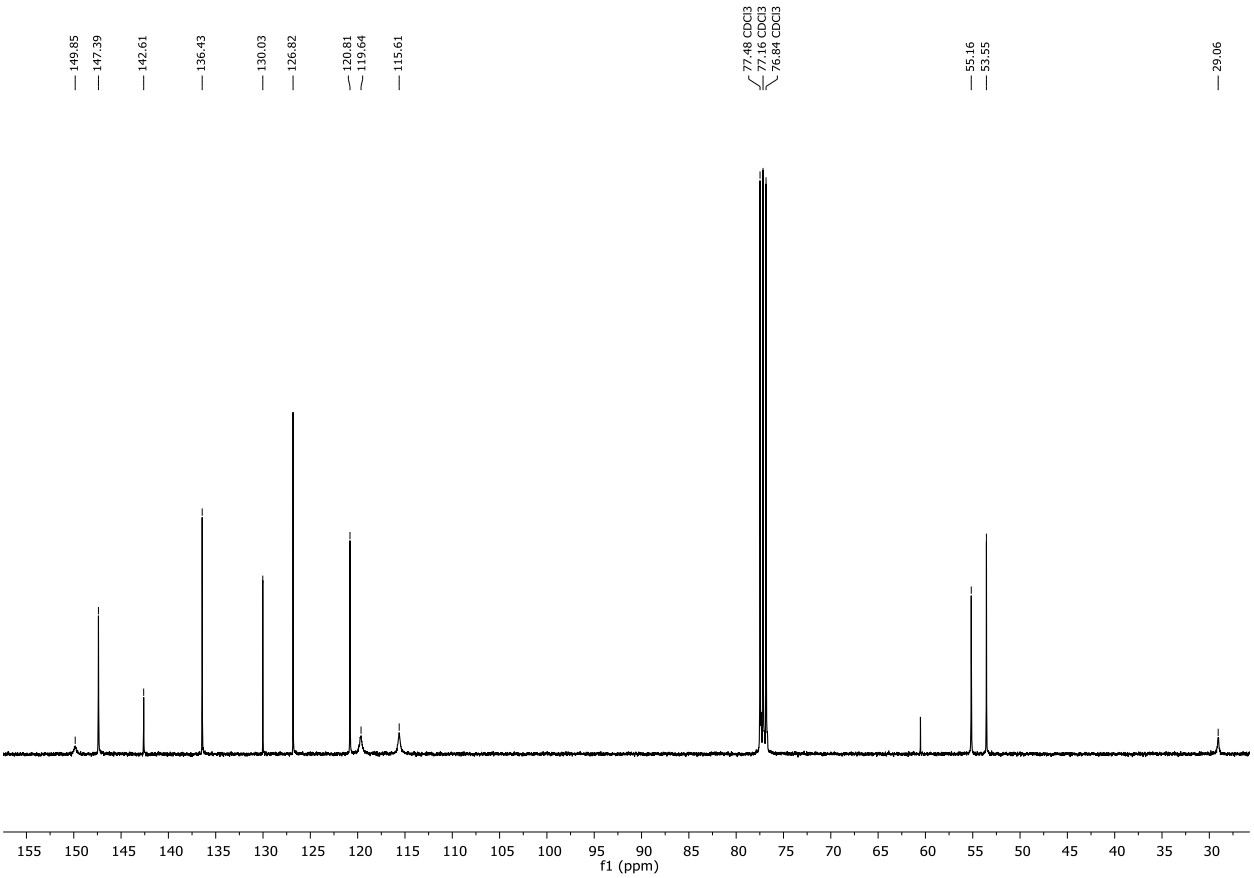


**Figure S2.** $^{13}C$ NMR spectrum of the $L^7BQ$ ligand collected in $CDCl_3$ under ambient conditions.

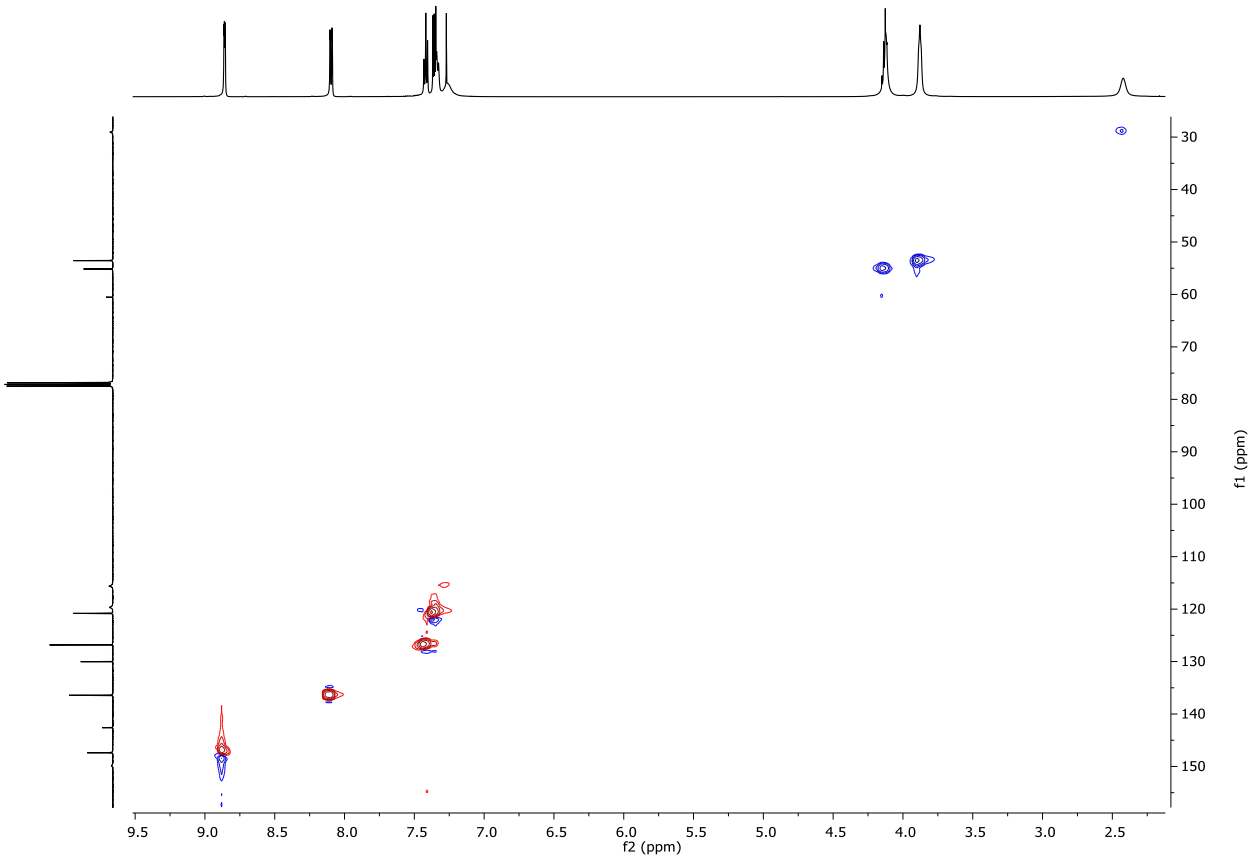


**Figure S3.** HSQC spectrum of the $L^7BQ$ ligand collected in $CDCl_3$ under ambient conditions.

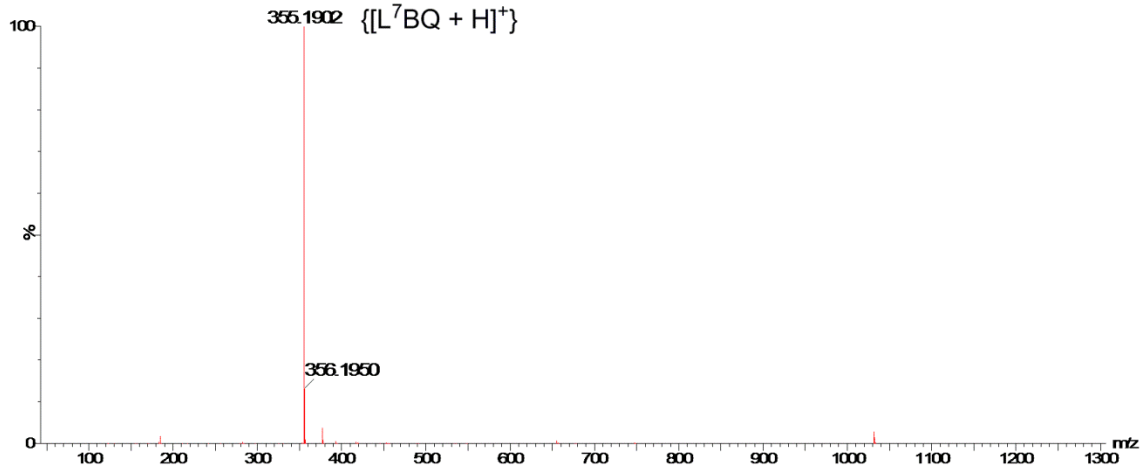


**Figure S4.** ESI-MS data showing the purified $L^7BQ$ ligand in acetonitrile.

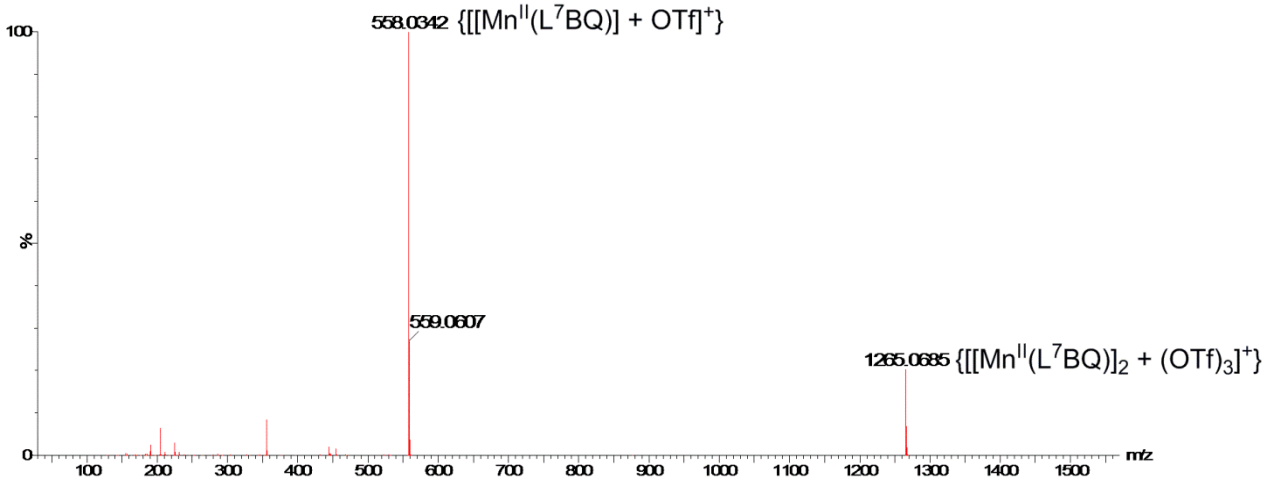


**Figure S5.** ESI-MS spectrum of $[Mn^{II}(L^7BQ)(OTf)_2]$ in acetonitrile.

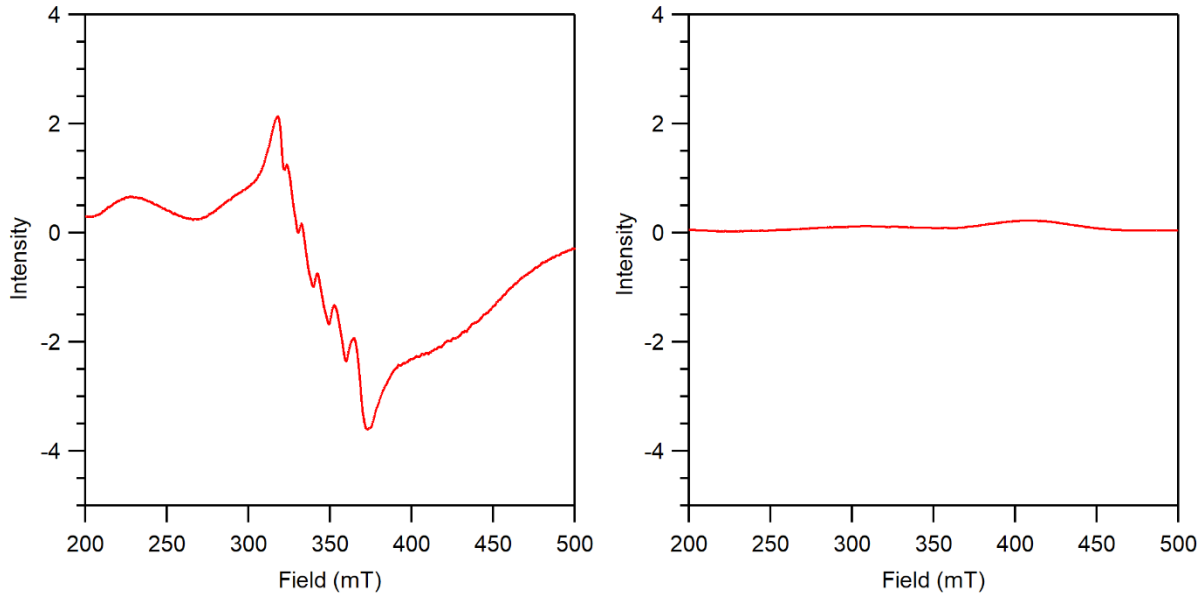


**Figure S6.** Perpendicular-mode (left) and parallel-mode (right) X-band EPR spectra of a 2.5 mM frozen MeCN solution of $[Mn^{II}(L^7BQ)(OTf)_2]$ collected at 5 K.

**Table S1.** Crystal Data and Structure Refinement for $[Mn^{II}(L^7BQ)(OTf)_2]$.

| | |
|---|---|
| Empirical formula | $C_{27}H_{25}F_6MnN_5O_6S_2$ |
| Formula weight | 748.58 |
| Temperature | 100(2) K |
| Wavelength | 1.54178 Å |
| Crystal system | Monoclinic |
| Space group[3] | $P2_1/n$ – alternate setting for $P2_1/c$ (No. 14 – $C_{2h}^5$) |
| Unit cell dimensions | **a** = 13.8379(4) Å **α** = 90.00° |
| | **b** = 14.1652(4) Å **β** = 105.211(1)° |
| | **c** = 16.3768(4) Å **γ** = 90.00° |
| Volume | 3097.66(15) $Å^3$ |
| Z | 4 |
| Density (calculated) | 1.605 $g/cm^3$ |
| Absorption coefficient | 5.51 $mm^{-1}$ |
| F(000) | 1524 |
| Crystal size | 0.24 x 0.18 x 0.10 $mm^3$ |
| Theta range for data collection | 3.73° to 69.49° |
| Index ranges | $-15 \leq h \leq 16$, $-17 \leq k \leq 17$, $-13 \leq l \leq 19$ |
| Reflections collected | 26589 |
| Independent reflections | 5484 [$R_{int}$ = 0.031] |
| Completeness to theta = 66.00° | 97.0 % |
| Absorption correction | Multi-scan |
| Max. and min. transmission | 1.000 and 0.787 |
| Refinement method | Full-matrix least-squares on $F^2$ |
| Data / restraints / parameters | 5484 / 0 / 525 |
| Goodness-of-fit on $F^2$ | 1.039 |
| Final R indices [5432 I>2sigma(I)] | $R_1$ = 0.0293, $wR_2$ = 0.0748 |
| R indices (all 5484 data) | $R_1$ = 0.0295, $wR_2$ = 0.0750 |
| Extinction coefficient | 0.00022(5) |
| Largest diff. peak and hole | 0.40 and -0.34 $e^-/Å^3$ |

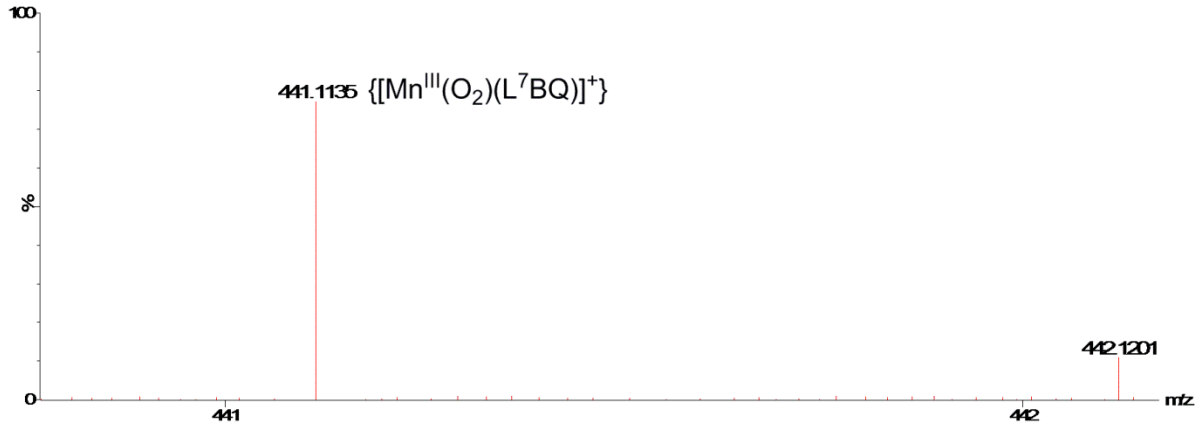


**Figure S7.** Low-temperature ESI-MS spectrum of $[Mn^{III}(O_2)(L^7BQ)]^+$ in acetonitrile.

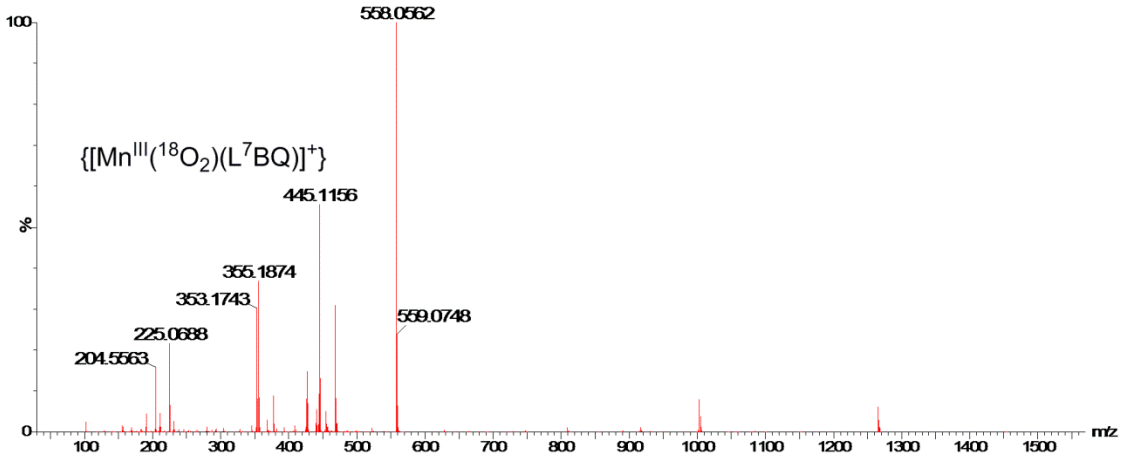


**Figure S8.** Low-temperature ESI-MS spectrum of $[Mn^{III}(^{18}O_2)(L^7BQ)]^+$ in acetonitrile. The major ion peak at 558.06 represents $[Mn^{II}(L^7BQ)(OTf)]^+$ (see Figure S5).

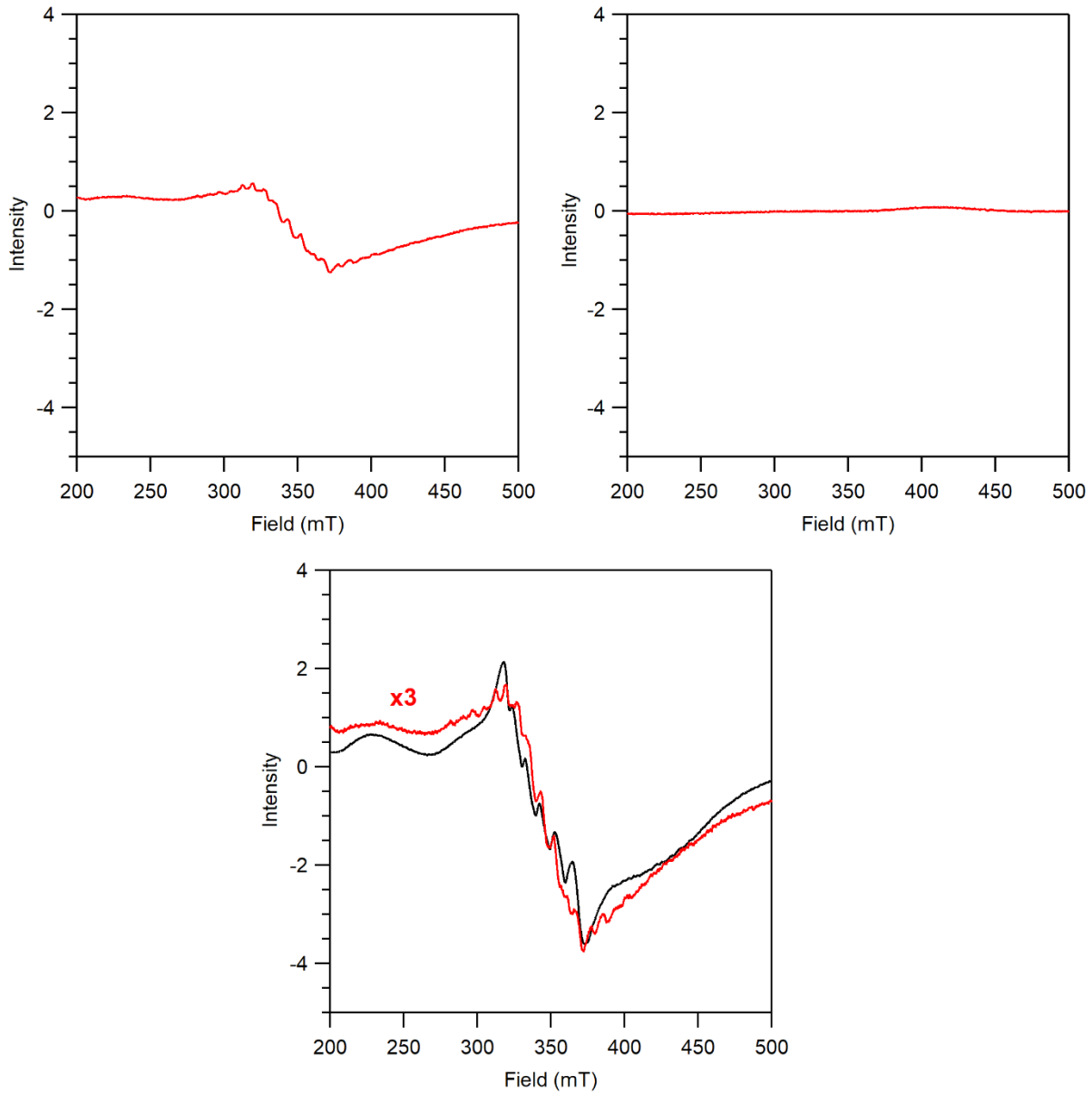


**Figure S9.** Perpendicular-mode (top left) and parallel-mode (top right) X-band EPR spectra of a 2.5 mM frozen MeCN solution of $[Mn^{III}(O_2)(L^7BQ)]^+$ collected at 5 K. Bottom panel: Overlay of perpendicular-mode X-band EPR spectra of $[Mn^{II}(L^7BQ)(OTf)_2]$ (black trace) and $[Mn^{III}(O_2)(L^7BQ)]^+$.

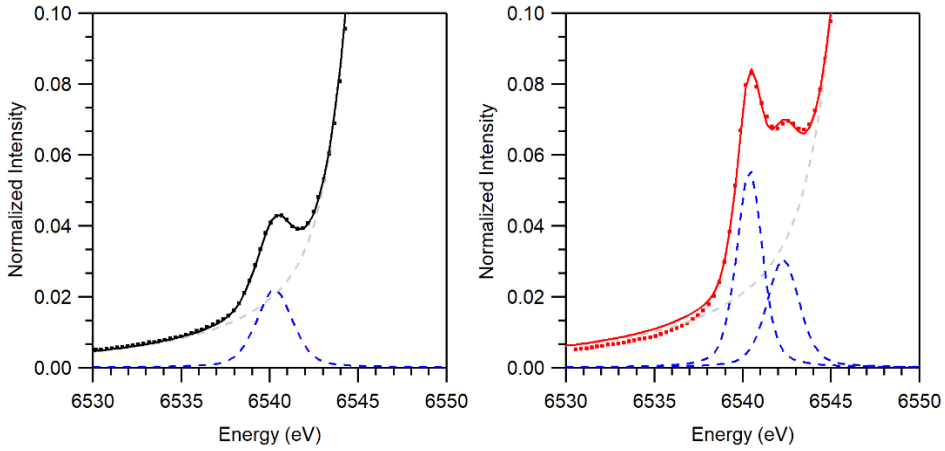


**Figure S10** Comparison of the normalized XAS pre-edge data (doted line) and fits (solid line) for $[Mn^{II}(L^{7}BQ)(OTf)_2]$ (left) and $[Mn^{III}(O_2)(L^{7}BQ)]^{+}$ (right). The fit of the background and the fit of the pre-edge features are represented by the dashed blue traces.

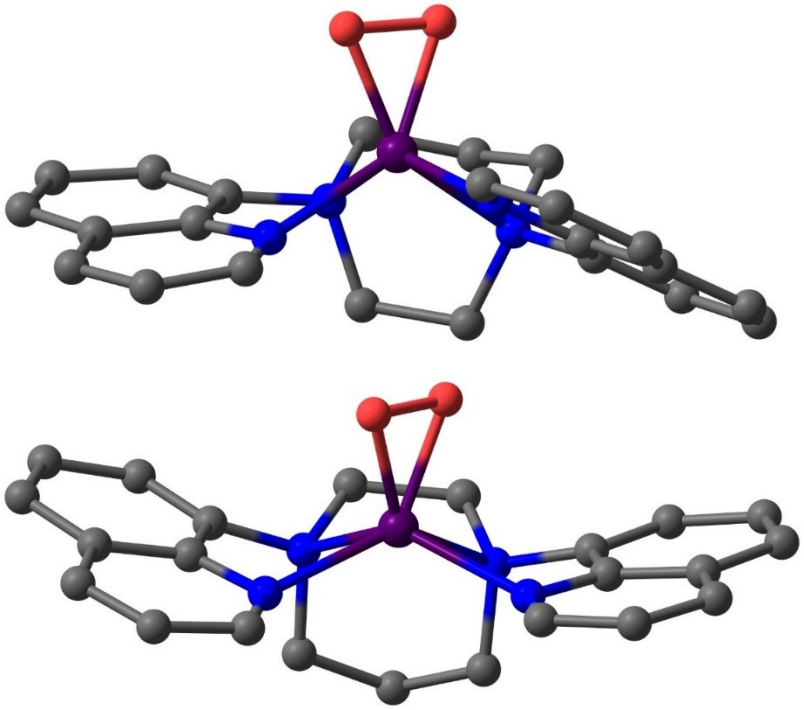

**Figure S11.** Structures for $[Mn^{III}(O_2)(L^7BQ)]^+$ with the peroxo bound propyl- and ethyl-linked faces of the $L^7BQ$ ligand (top and bottom, respectively).

**Table S2.** Selected Geometric Parameters for $[Mn^{III}(O_2)(L^7BQ)]^+$ with the Peroxo Bound to the Propyl-linked Face of the $L^7BQ$ ligand (Figure S11, top).

| Bond Length (Å) | | | |
|---|---|---|---|
| Mn–O1 | 1.862 | Mn–N1 | 2.142 |
| Mn–O2 | 1.856 | Mn–N2 | 2.315 |
| O1-O2 | 1.418 | Mn–N3 | 2.204 |
| | | Mn–N4 | 2.199 |

| Bond Angle (°) | | | |
|---|---|---|---|
| N1–Mn–O1 | 96.85 | N1–Mn–N2 | 74.38 |
| N2–Mn–O1 | 109.11 | N1–Mn–N3 | 116.37 |
| N3–Mn–O1 | 145.28 | N1–Mn–N4 | 98.66 |
| N4–Mn–O1 | 107.62 | N2–Mn–N3 | 73.10 |
| N1–Mn–O2 | 140.96 | N2–Mn–N4 | 143.17 |
| N2–Mn–O2 | 107.32 | N3–Mn–N4 | 78.46 |
| N3–Mn–O2 | 100.67 | O1–Mn–O2 | 44.83 |
| N4–Mn–O2 | 100.47 | | |

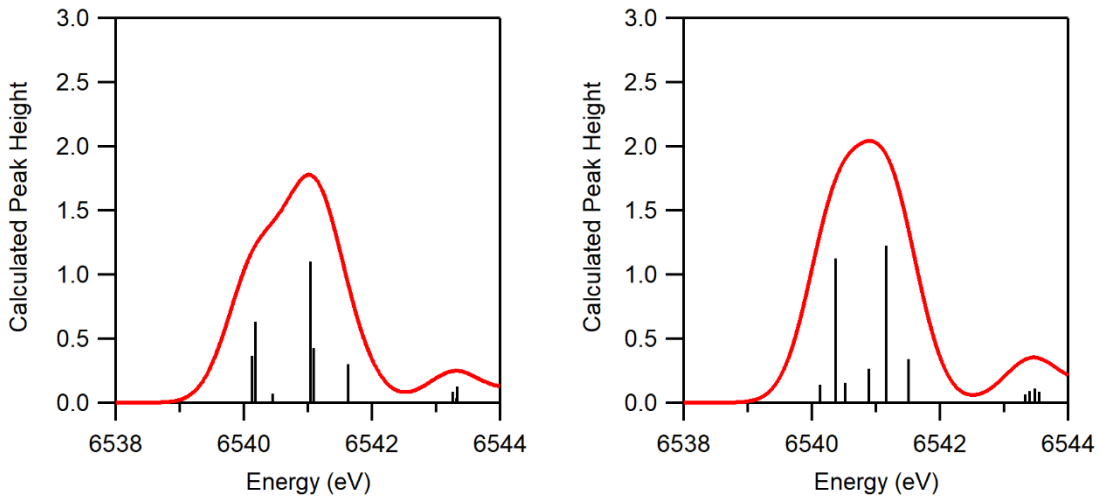


**Figure S12.** TD-DFT simulated pre-edge spectra with vertical lines showing transitions for $[Mn^{III}(O_2)(L^7BQ)]^+$ with the peroxo bound to the propyl-linked (left) and ethyl-linked faces (right) of the $L^7BQ$ ligand (see Figure S11). The simulated spectra employed Gaussian functions with a 1 eV bandwidth.

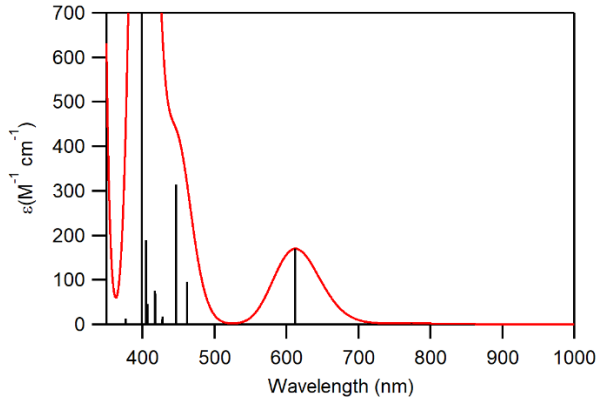


**Figure S13.** TD-DFT simulated UV-Vis absorption spectra with vertical lines showing transitions for the $[Mn^{III}(O_2)(L^7BQ)]^+$ with the peroxo bound to the propyl-linked face of the $L^7BQ$ ligand (Figure S11, top). The transition at 612 nm corresponds to a transition involving a one-electron excitation from the $Mn^{III}$ α-$3d_z^2$ to α-$3d_{xy}$ MO.

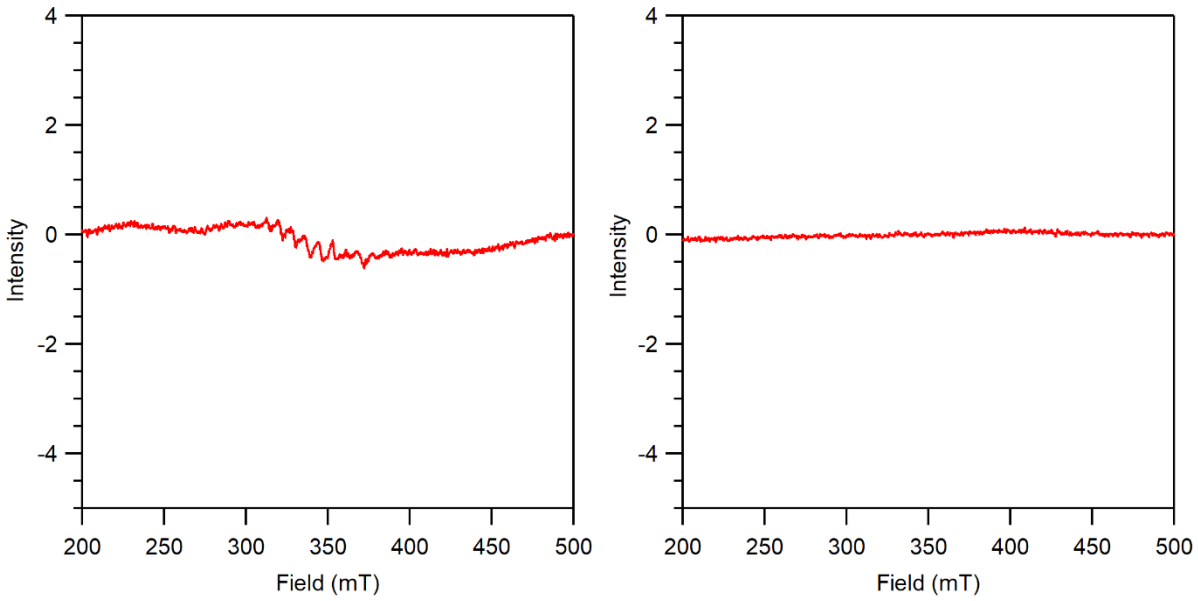


**Figure S14.** 10 K perpendicular- (left) and parallel-mode (right) X-band EPR spectra of a 2.5 mM frozen MeCN solution of the self-decay product of $[Mn^{III}(O_2)(L^7BQ)]^+$.

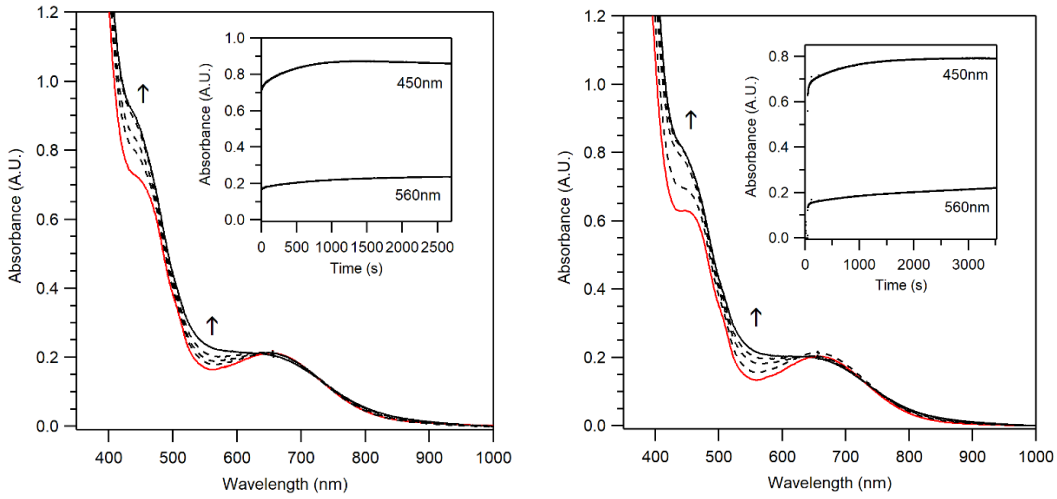


**Figure S15.** Left: Electronic absorption changes flowing the addition of 1.0 equivalents of $[Mn^{II}(L^7BQ)(OTf)_2]$ to $[Mn^{III}(O_2)(L^7BQ)]^+$ at -40°C in MeCN (the red and black traces are of the initial and final spectra, respectively). Right: Self decay of $[Mn^{III}(O_2)(L^7BQ)]^+$ at -40°C in MeCN (the red and black traces are of the initial and final spectra, respectively).

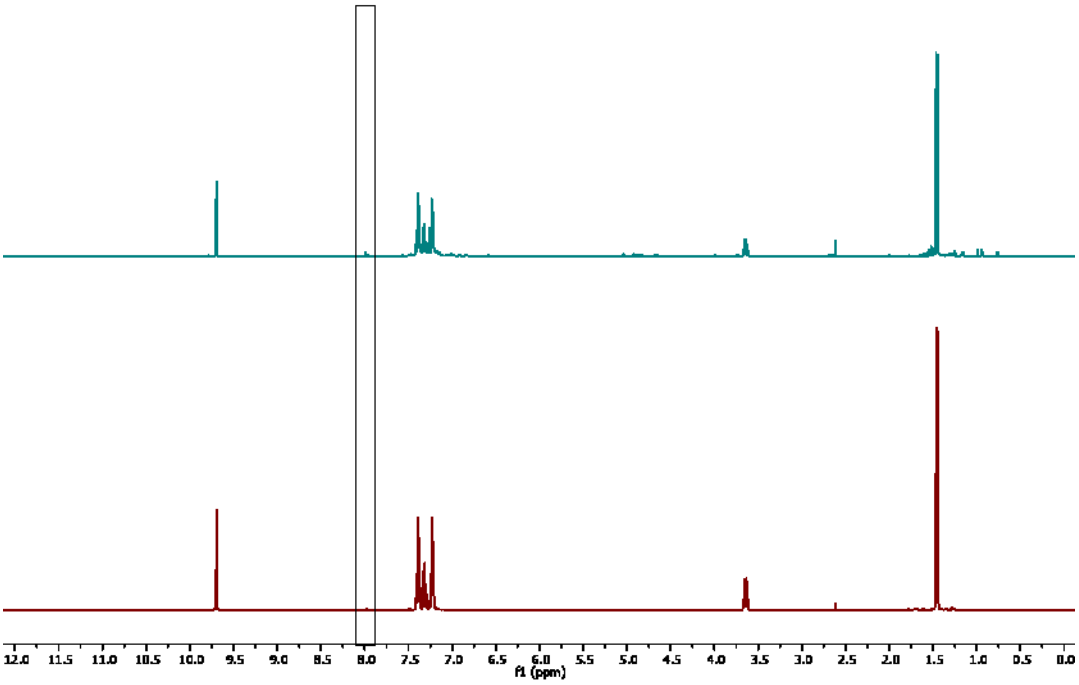


**Figure S16.** $^{1}$H NMR spectra of PPA. Top: Spectrum of PPA with acid impurity at ~8.0 ppm. Bottom: Spectrum of fresh PPA with no acid impurity present.

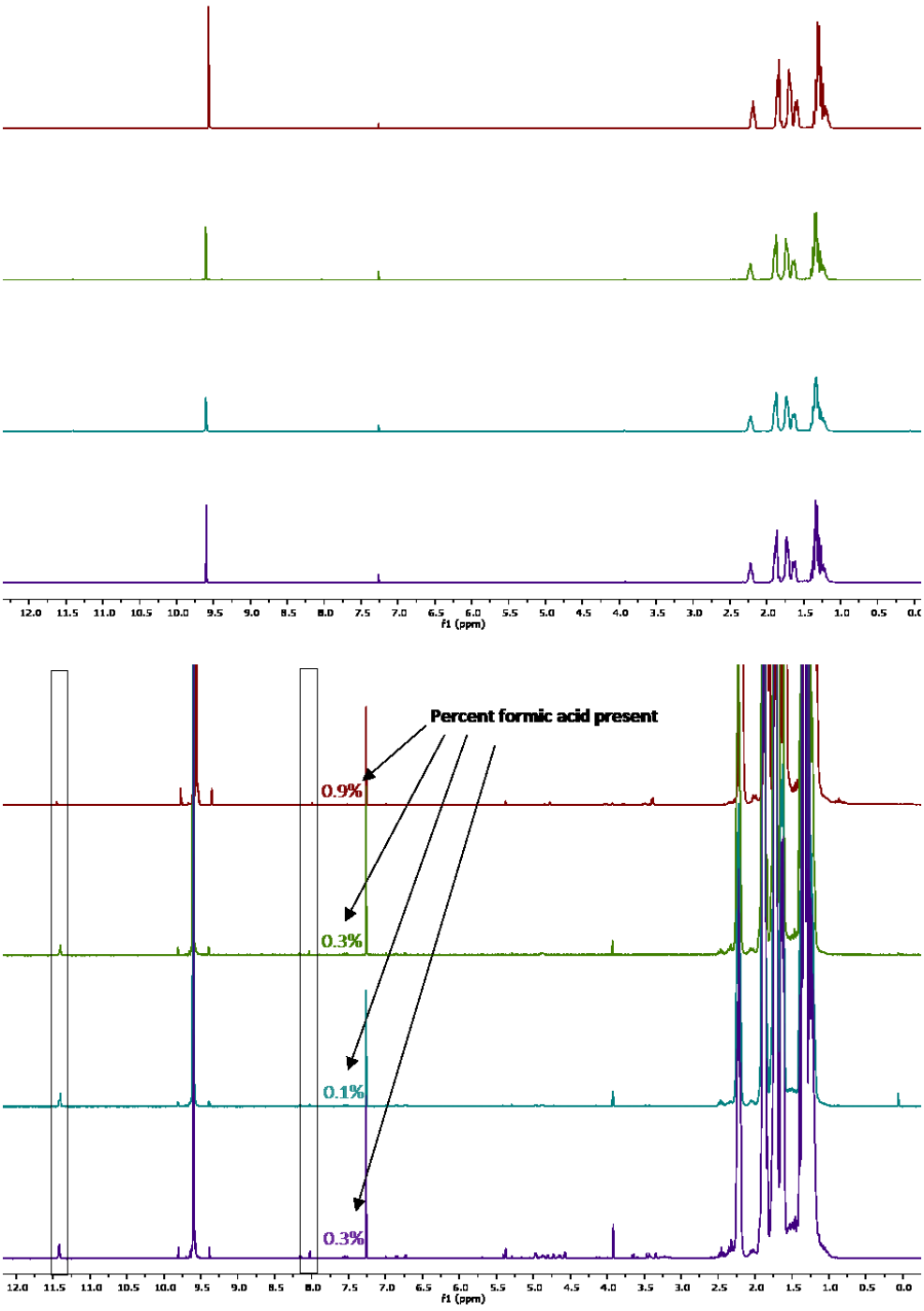


**Figure S17.** $^{1}$H NMR spectra of CCA. The top red trace is of as-received CCA, while the other spectra are of CCA following distillation. Top: Complete spectra showing all resonances. Bottom: Expanded view spectra showing the resonances from acid impurities at 11.4 ppm and 8.0 ppm, which are attributed to cyclohexanecarboxylic acid and formic acid, respectively. The percentage of formic acid present was determined by integrating this peak relative to the aldehyde peak for CCA.

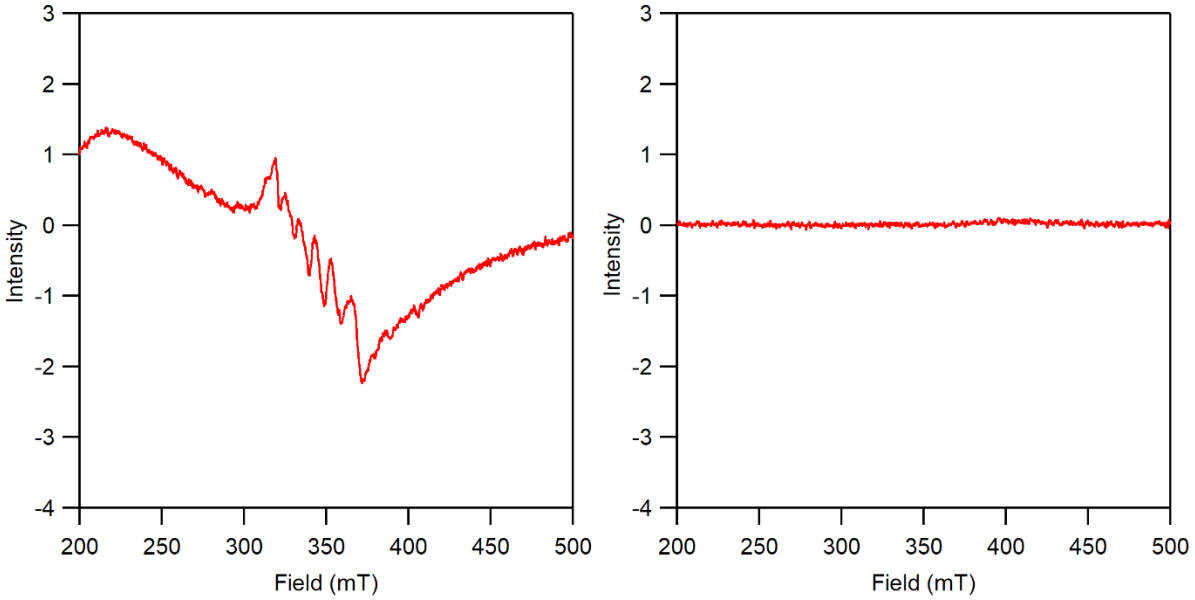


**Figure S18.** Perpendicular- (left) and parallel-mode (right) EPR spectra of $[Mn^{III}(O_2)(L^7BQ)]^+$ following the addition of cyclohexanecarboxylic acid.

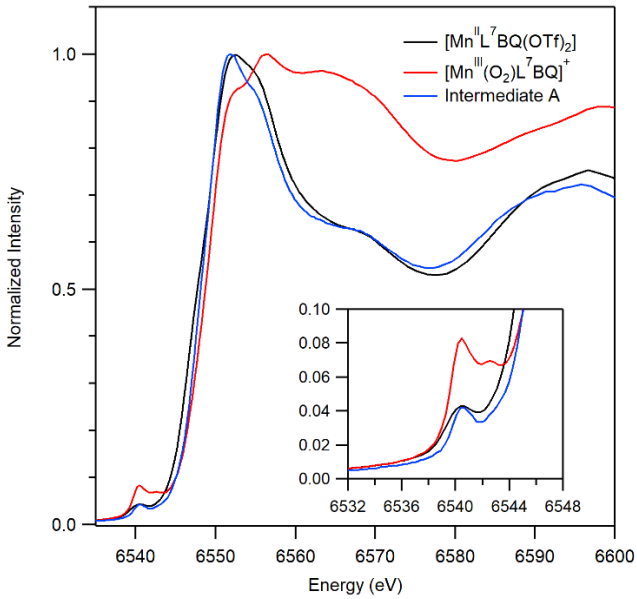


**Figure S19.** Comparison of X-ray absorption near edge structures of $[Mn^{III}(O_2)(L^7BQ)(OTf)_2]$ (black trace), $[Mn^{III}(O_2)(L^7BQ)]^+$ (red trace), and intermediate A (blue trace).

**Table S3.** Cartesian Coordinates for the DFT-optimized Structure of $[Mn^{III}(O_2)L^7BQ]^+$ with the Peroxo Bound on the Propyl-linked Face of the $L^7BQ$ Ligand (Figure S11, top).

| | X | Y | Z |
|---|---|---|---|
| Mn | -0.077993318 | 0.052291708 | -0.037042407 |
| O | -1.757596085 | -0.741539254 | 0.092921937 |
| O | -1.825512281 | 0.673309256 | 0.033004256 |
| N | 1.035216752 | -1.752786393 | -0.335699992 |
| N | 0.575766014 | 0.083285091 | -2.257622547 |
| N | 1.013750677 | 1.940454871 | -0.357466111 |
| N | 0.595304826 | 0.522698532 | 2.002320454 |
| C | 1.443193890 | -2.576903757 | 0.614102789 |
| C | 1.659912611 | -3.951873470 | 0.387104270 |
| C | 1.385059536 | -4.475928812 | -0.859040416 |
| C | 0.947859113 | -3.618150484 | -1.902214936 |
| C | 0.832923402 | -2.230854116 | -1.602619120 |
| C | 0.488223693 | -1.298642774 | -2.628056676 |
| C | -0.315144102 | 1.017562870 | -2.981807963 |
| C | -0.003435419 | 2.469140515 | -2.625758459 |
| C | 0.096713492 | 2.834878724 | -1.147220821 |
| C | 0.357044357 | -0.185020475 | 3.090251727 |
| C | 0.672490619 | 0.273188284 | 4.387549862 |
| C | 1.246213480 | 1.517976689 | 4.530210227 |
| C | 1.499281916 | 2.312421497 | 3.381124056 |
| C | 1.147392274 | 1.765572903 | 2.108296136 |
| C | 1.363830003 | 2.531678682 | 0.927202150 |
| C | 2.252225998 | 1.583811102 | -1.108476050 |
| C | 1.990066297 | 0.547424868 | -2.226471999 |
| C | 0.615679737 | -4.067462715 | -3.209823560 |
| C | 0.200860867 | -3.161449880 | -4.162543166 |
| C | 0.151673841 | -1.771053063 | -3.880919797 |
| C | 2.071642674 | 3.609739212 | 3.445929219 |
| C | 2.282171609 | 4.329012804 | 2.288744520 |
| C | 1.928993421 | 3.787721100 | 1.028866096 |
| H | 1.593951725 | -2.151206061 | 1.607212378 |
| H | 2.008665290 | -4.580286799 | 1.207462359 |
| H | 1.498770730 | -5.544509661 | -1.056192280 |
| H | -0.194428717 | 0.909258808 | -4.072261823 |
| H | -1.350142304 | 0.752838247 | -2.725130538 |
| H | 0.919130610 | 2.780322667 | -3.137955469 |
| H | -0.799558248 | 3.095913395 | -3.056022426 |
| H | -0.883514335 | 2.800971692 | -0.655101855 |
| H | 0.461238828 | 3.870506118 | -1.091183067 |
| H | -0.109523286 | -1.163038458 | 2.950708745 |
| H | 0.456681024 | -0.360819507 | 5.248506958 |
| H | 1.506228425 | 1.908746571 | 5.516805115 |
| H | 2.718324260 | 2.492459768 | -1.518871528 |
| H | 2.948281409 | 1.158514522 | -0.375924872 |
| H | 2.265804157 | 0.947694010 | -3.213939501 |
| H | 2.624025933 | -0.326293867 | -2.048348291 |
| H | 0.690508046 | -5.132557873 | -3.439796055 |
| H | -0.067409773 | -3.504787488 | -5.164067732 |
| H | -0.130552790 | -1.079389823 | -4.674721125 |
| H | 2.337937895 | 4.022493761 | 4.421523570 |
| H | 2.724539976 | 5.326277493 | 2.332091016 |
| H | 2.112710533 | 4.379401061 | 0.130621583 |

**Table S4.** Cartesian Coordinates for the DFT-optimized Structure of $[Mn^{III}(O_2)L^7BQ]^+$ with the Peroxo Bound on the Ethyl-linked Face of the $L^7BQ$ Ligand (Figure S11, bottom).

| | X | Y | Z |
|---|---|---|---|
| Mn | 0.000000000 | 0.000000000 | 0.000000000 |
| O | 1.735718240 | 0.000000000 | 0.694846300 |
| O | 1.735718240 | 0.000000000 | -0.711695357 |
| N | -0.465025601 | 2.116366370 | 0.456228537 |
| N | -0.869168113 | -0.056669920 | 2.060354374 |
| N | -0.960207236 | -2.061479980 | 0.352805697 |
| N | -0.820911559 | -0.596390625 | -1.904218033 |
| C | -0.386078425 | 3.153416070 | -0.356336573 |
| C | -0.138743204 | 4.467151097 | 0.098316826 |
| C | 0.072335652 | 4.677597180 | 1.444277985 |
| C | 0.005555143 | 3.582989941 | 2.346681254 |
| C | -0.303426365 | 2.302354474 | 1.801428673 |
| C | -0.415996020 | 1.172530766 | 2.664907990 |
| C | -2.373464777 | -0.038347048 | 2.026840748 |
| C | -2.972638606 | -1.393357667 | 1.698967910 |
| C | -2.456138525 | -2.016053590 | 0.416088047 |
| C | -0.944281441 | 0.148756046 | -2.987542222 |
| C | -0.868771407 | -0.384505155 | -4.292619363 |
| C | -0.599677032 | -1.727617635 | -4.452838617 |
| C | -0.457163403 | -2.558103543 | -3.309476110 |
| C | -0.626630171 | -1.947047490 | -2.034959780 |
| C | -0.575477142 | -2.740187787 | -0.849365824 |
| C | -0.336098896 | -2.479348630 | 1.620296424 |
| C | -0.325670272 | -1.305579969 | 2.650449435 |
| C | 0.245863139 | 3.699933770 | 3.742738977 |
| C | 0.177730647 | 2.584696507 | 4.550676700 |
| C | -0.168602380 | 1.318168789 | 4.014373295 |
| C | -0.148169600 | -3.944886945 | -3.368319879 |
| C | -0.027740647 | -4.677038028 | -2.205250074 |
| C | -0.263526028 | -4.081080224 | -0.939147809 |
| H | -0.505354113 | 2.956739824 | -1.424244645 |
| H | -0.095723666 | 5.285028355 | -0.622146453 |
| H | 0.297495904 | 5.675295762 | 1.828523136 |
| H | -2.740889332 | 0.289511700 | 3.012418804 |
| H | -2.676058704 | 0.718605518 | 1.288949157 |
| H | -2.837175707 | -2.084225758 | 2.543747816 |
| H | -4.060667641 | -1.261994399 | 1.594800808 |
| H | -2.804678364 | -1.445984966 | -0.455607758 |
| H | -2.845131178 | -3.043902313 | 0.322528505 |
| H | -1.089838024 | 1.220565154 | -2.837812520 |
| H | -0.992460013 | 0.279018688 | -5.149344854 |
| H | -0.492016471 | -2.163632710 | -5.448812782 |
| H | -0.845684000 | -3.355797041 | 2.050802786 |
| H | 0.697289572 | -2.767144157 | 1.395808012 |
| H | -0.884509342 | -1.584742669 | 3.555498948 |
| H | 0.709187376 | -1.101234416 | 2.943938973 |
| H | 0.488855369 | 4.680695502 | 4.157377311 |
| H | 0.371269625 | 2.669546340 | 5.622168774 |
| H | -0.255902413 | 0.461028663 | 4.683803081 |
| H | -0.005932087 | -4.414175929 | -4.344173149 |
| H | 0.220909722 | -5.739575389 | -2.250195743 |
| H | -0.222999309 | -4.696413243 | -0.038757932 |